DOI: 10.1002/chem.200701720

Light-Harvesting Supramolecular Porphyrin Macrocycle Accommodating a Fullerene–Tripodal Ligand

Yusuke Kuramochi,[a] Akiharu Satake,[a] Mitsunari Itou,[b] Kazuya Ogawa,[a] Yasuyuki Araki,[b] Osamu Ito,[b] and Yoshiaki Kobuke*[a, c]

Abstract: Trisporphyrinatozinc(II) (**1**–Zn) with imidazolyl groups at both ends of the porphyrin self-assembles exclusively into a light-harvesting cyclic trimer (N-(**1**–Zn)$_3$) through complementary coordination of imidazolyl to zinc(II). Because only the two terminal porphyrins in **1**–Zn are employed in ring formation, macrocycle N-(**1**–Zn)$_3$ leaves three uncoordinated porphyrinatozinc(II) groups as a scaffold that can accommodate ligands into the central pore. A pyridyl tripodal ligand with an appended fullerene connected through an amide linkage (C_{60}–Tripod) was synthesized by coupling tripodal ligand **3** with pyrrolidine-modified fullerene, and this ligand was incorporated into N-(**1**–Zn)$_3$. The binding constant for C_{60}–Tripod in benzonitrile reached the order of $10^8\,M^{-1}$. This value is ten times larger than those of pyridyl tetrapodal ligand **2** and tripodal ligand **3**. This behavior suggests that the fullerene moiety contributes to enhance the binding of C_{60}–Tripod in N-(**1**–Zn)$_3$. The fluorescence of N-(**1**–Zn)$_3$ was almost completely quenched ($\approx$97%) by complexation with C_{60}–Tripod, without any indication of the formation of charge-separated species or a triplet excited state of either porphyrin or fullerene in the transient absorption spectra. These observations are explained by the idea that the fullerene moiety of C_{60}–Tripod is in direct contact with the porphyrin planes of N-(**1**–Zn)$_3$ through fullerene–porphyrin π–π interactions. Thus, C_{60}–Tripod is accommodated in N-(**1**–Zn)$_3$ with a π–π interaction and two pyridyl coordinations. The cooperative interaction achieves a sufficiently high affinity for quantitative and specific introduction of one equivalent of tripodal guest into the antenna ring, even under dilute conditions ($\approx 10^{-7}$ M) in polar solvents such as benzonitrile. Additionally, complete fluorescence quenching of N-(**1**–Zn)$_3$ when accommodating C_{60}–Tripod demonstrates that all of the excitation energy collected by the nine porphyrins migrates rapidly over the macrocycle and then converges efficiently on the fullerene moiety by electron transfer.

Keywords: fullerenes · photochemistry · photosynthesis · porphyrinoids · self-assembly

Introduction

Photosynthetic organisms have developed characteristic light-harvesting antenna (LH) systems to capture weak energy from sunlight and efficiently transfer it to the reaction center (RC).[1] LH systems in purple bacteria, in particular, have been extensively studied and fully characterized. Purple bacteria have two types of cyclic antenna, LH1[2] and LH2.[3] They operate in biological membranes to transport the energy captured by LH2 to the RC located in LH1 with

[a] Dr. Y. Kuramochi, Prof. A. Satake, Prof. K. Ogawa, Prof. Y. Kobuke
Graduate School of Materials Science
Nara Institute of Science and Technology
Takayama 8916-5, Ikoma
Nara 630-0101 (Japan)
E-mail: kobuke@iae.kyoto-u.ac.jp

[b] Dr. M. Itou, Prof. Y. Araki, Prof. O. Ito
Institute of Multidisciplinary Research for Advanced Materials
Tohoku University, Katahira
Sendai, 980-8577 (Japan)

[c] Prof. Y. Kobuke
Present address: Institute of Advanced Energy
Kyoto University, Gokasho
Uji, Kyoto 611-0011 (Japan)
Fax: (+81) 774-38-3508

Supporting information for this article is available on the WWW under http://www.chemeurj.org/ or from the author. It contains MALDI-TOF mass spectral and GPC analyses of C-(**1**–Zn)$_3$, GPC analyses of **9** and **10**; an HMQC spectrum of N-(**1**–Zn)$_3$, Q band curve fitting of N-(**1**–Zn)$_3$ by N-(**5**–Zn)$_2$ and **6**–Zn, UV/Vis titration spectra of **2** in benzonitrile, time-resolved spectra (fluorescence decay and transient absorption) of the complex of N-(**1**–Zn)$_3$ and C_{60}-Tripod, and ^{1}H and ^{13}C NMR spectra of C_{60}-Tripod.

high efficiency.[4] Excitation of the special pair initiates charge separation followed by multistep electron-transfer reactions in the RC to give a transmembrane proton gradient that is coupled with adenosine triphosphate (ATP) production through an ATP-synthase enzyme.[1] This is the primary energy source of all of the living organisms on earth, and application of the photosynthetic-energy-conversion system has great potential to resolve energy and environmental problems in the world.

A number of researchers have attempted to construct artificial light-harvesting systems by covalent[5,6] or noncovalent[5,7] approaches. Both approaches provide important contributions not only to understanding the natural system, but also in creating efficient energy-harvesting systems. The noncovalent self-assembly approach has the merit of using simple construction units with minimum synthetic effort. It also allows us to mimic the sophisticated construction principles of nature.

Mimicking the RC is also important for further conversion of the captured energy into electrochemical potential. Fullerene has been widely used for various synthetic porphyrin models as an electron acceptor because of its small reorganization energy (λ) in photoinduced electron-transfer reactions.[8,9] In these studies, the porphyrin and the fullerene units were also connected through either covalent[9] or noncovalent linkers.[10] Polar solvents, such as benzonitrile, are often used in the study of photoinduced electron transfer of covalently linked systems because they stabilize the charge-separated species and can maintain a long-lived charge-separated state. However, the use of polar solvents produces difficulties for noncovalent linker systems because coordination and hydrogen-bonding interactions are weakened, which leads to cleavage of the conjugates in polar solvents. To overcome this difficulty, multipoint binding between the porphyrin and the fullerene units was used,[10f] but addition of excess amounts of ligand was necessary to obtain significant amounts of the porphyrin–fullerene conjugate in benzonitrile.

We previously reported that bis(imidazolylporphyrinatozinc) linked through an *m*-phenylene or *m*-bis(ethynylene)-phenylene moiety afforded a macrocyclic hexamer and pentamer by complementary coordination of imidazolyl to zinc(II) (Figure 1).[11,12,13] These macrocycles mimicked the structure of LH2 and achieved rapid energy transfer in porphyrinic pigments without losing their fluorescence properties.[12,14] In a previous communication,[15] this supramolecular methodology was applied to **1**–Zn, which had imidazolyl groups at both porphyrin ends and exclusively gave macrocyclic trimer N-(**1**–Zn)$_3$ (Figure 1). In this macrocycle, the two terminal porphyrins in **1**–Zn participated in ring-forming complementary coordinations, and the uncoordinated central porphyrinatozinc(II) provided the scaffold to specifically accommodate a ligand, such as tetrakis{4-[(4-pyridyl)-ethynyl]phenyl}methane (**2**), in the pore of N-(**1**–Zn)$_3$ by three-point coordination from pyridyl to the zinc moieties. In composite **2**/N-(**1**–Zn)$_3$, ligand **2** possesses a fourth arm

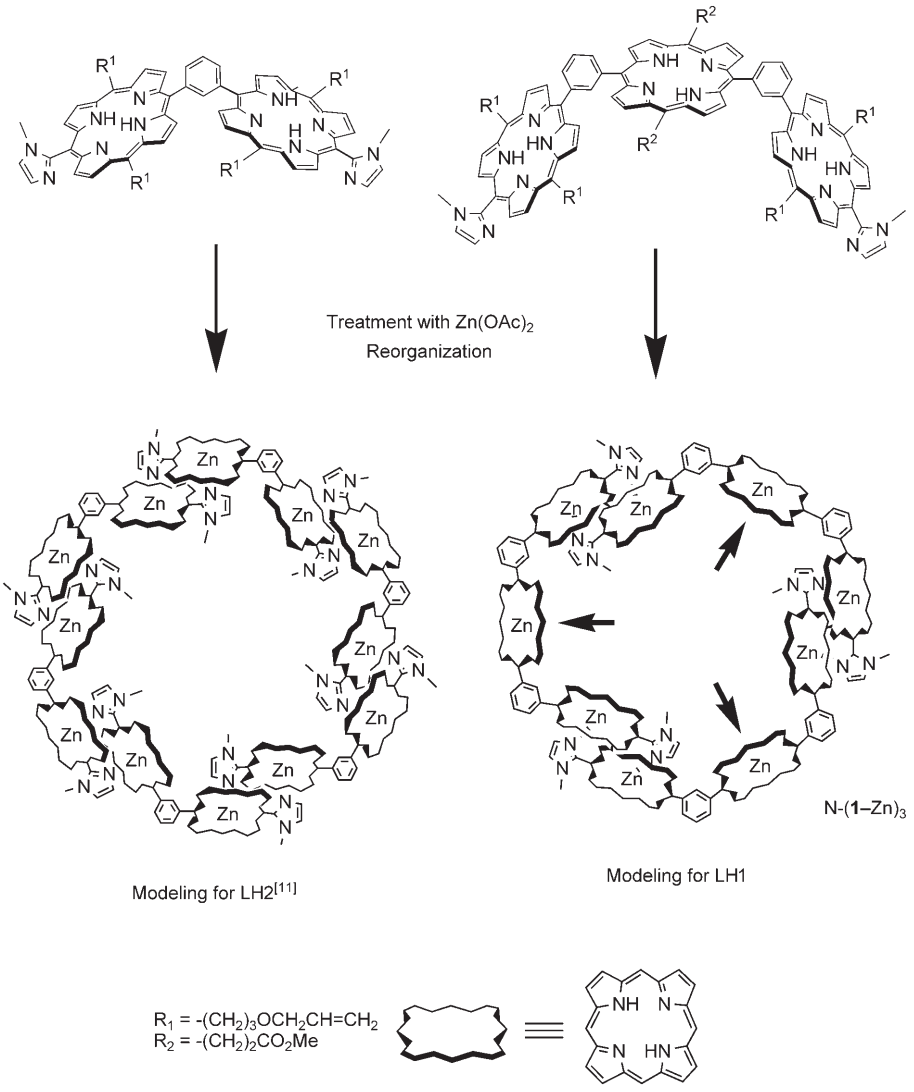

Figure 1. Structures of the porphyrin macrocycles. Arrows indicate the uncoordinated porphyrinatozinc sites.

that does not participate in conjugate formation and can be modified with energy or an electron-acceptor unit. Although various types of light-harvesting and RC models that use porphyrins and electron-acceptor molecules have been reported independently, their combined architectures have been constructed in only a limited number of cases to date.[16] Herein, we report the synthesis of a fullerene–tripodal ligand (C_{60}–Tripod) by modifying one arm of the tetrapodal ligand with a fullerene moiety (Figure 2) and incorporated it into N-(**1**–Zn)$_3$ with three-point binding of the pyridyl to the zinc moieties. The multipoint binding enabled us to investigate the photochemical properties of the antenna/electron acceptor composite, even in benzonitrile. Herein we also describe detailed structural studies of the free-base trisporphyrin (**1**), ring formation behavior of **1**–Zn, and the incorporation of trispyridine derivatives into N-(**1**–Zn)$_3$.

Results

Synthesis of 1: Free base **1** was synthesized by two porphyrin condensation reactions based on Lindsey's method (Scheme 1).[17] The first condensation of 1-methylimidazole-2-carboxaldehyde, 3-(4,4-dimethyl-2,6-dioxane-1-yl)benzaldehyde, and *meso*-(3-allyloxypropyl)dipyrromethane afforded monomeric porphyrin **5** in a yield of 13%[11c] accompanied by two porphyrin by-products, bis(3-(4,4-dimethyl-2,6-dioxan-1-yl)phenyl)porphyrin **6** and bis(1-methylimidazol-2-yl)porphyrin. Porphyrin by-product **6** was also isolated for use as the reference material. The second condensation of **4**, which was obtained by deprotecting **5**, and *meso*-methoxycarbonylethyldipyrromethane[18] gave **1** in a yield of 24% (based on **4**). Because the second condensation did not afford porphyrin by-products except for tarry materials, the purification of **1** was easily achieved by means of silica gel column chromatography.

The ^{1}H NMR spectrum of **1** in $CDCl_3$ showed signals of a slightly complex nature (Figure 3). The Im-4, Im-5, and N-Me protons had four nonequivalent signals (at $\delta = 7.681$, 7.677, 7.65, and 7.64 ppm for Im-4; 7.47, 7.45, 7.44, and 7.41 ppm for Im-5; 3.40, 3.37, 3.36, and 3.30 ppm for N-Me, respectively) with the same integration values. On the other hand, the Ph-2 protons had six nonequivalent signals between $\delta = 8.97$ and 9.13 ppm, in which the two signals indicated by ● had an integration value twice as large as the four signals indicated by ○. Because each porphyrin is oriented perpendicularly to the *m*-phenylene and *N*-methylimidazolyl moieties to reduce steric hindrance, there is a possibility that **1** has several atropisomers unless free rotation is allowed. These nonequivalent signals for the imidazolyl and phenyl moieties suggest the existence of their isomers.

Synthesis of C_{60}–Tripod: The tripodal ligand C_{60}–Tripod, which is connected to a fullerene moiety through amide bonding, was synthesized according to Scheme 2. 4-(Triphenylmethyl)benzoic acid was synthesized according to a published procedure.[19] The iodination of 4-(triphenylmethyl)-benzoic acid was carried out by using bis(trifluoroacetoxy)iodobenzene (5 equiv) and I_2 (5 equiv) at 60 °C in CCl_4 to give a mixture of **7** and tetraiodo-substituted **7** in a molar ratio of 1:1. When smaller equivalents of bis(trifluoroacetoxy)iodobenzene (2.5 equiv) and I_2 (2.5 equiv) were used, a mixture of **7** and the *meta*-iodo compound (see Scheme S1 in the Supporting Information) was formed in a molar ratio

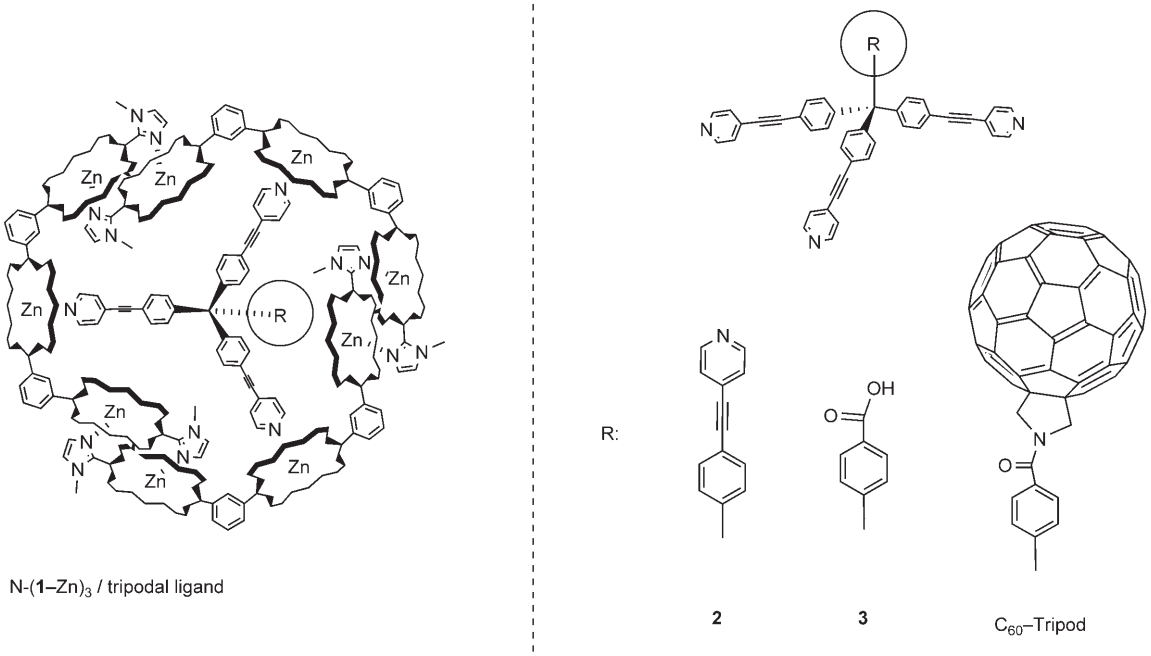

Figure 2. Structures of tripodal ligands **2**, **3**, and C_{60}–Tripod.

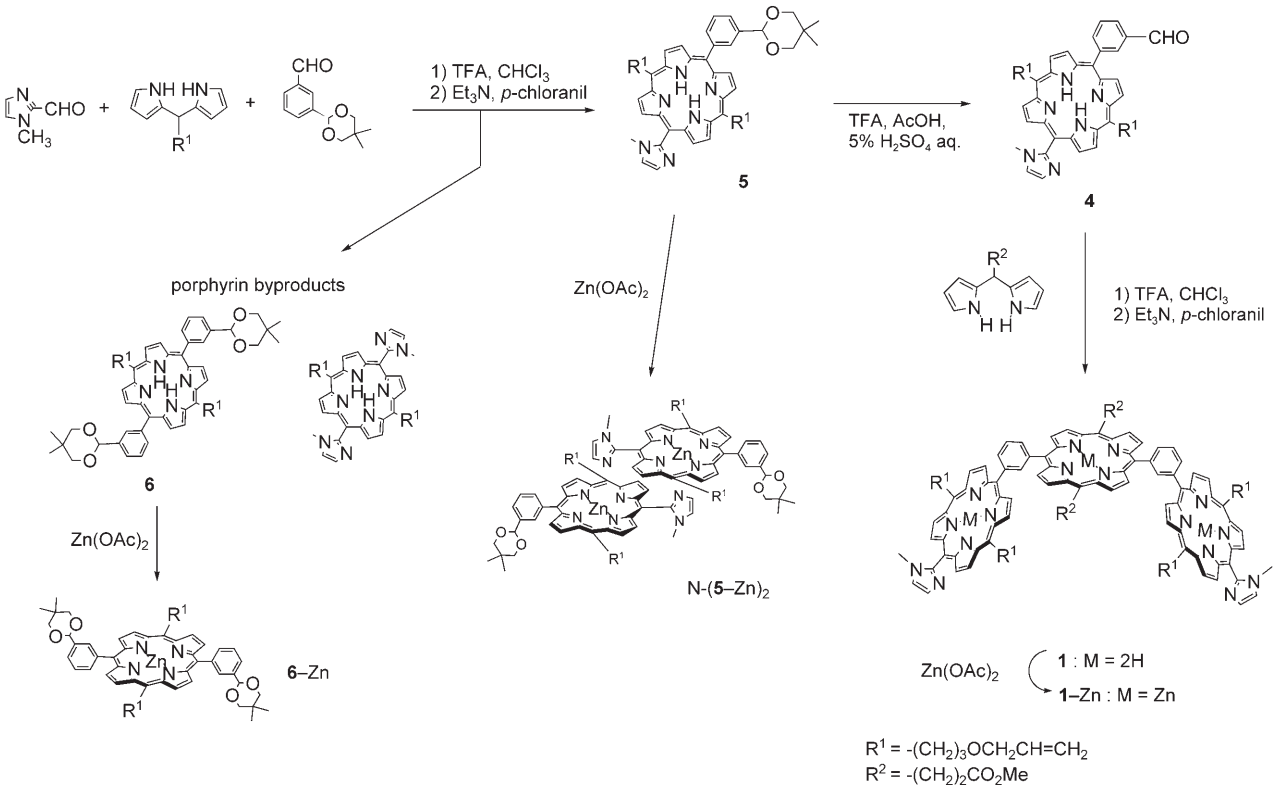

Scheme 1. Synthetic routes for trisporphyrin **1**–Zn, reference dimer N-(**5**–Zn)$_2$, and monomer **6**–Zn.

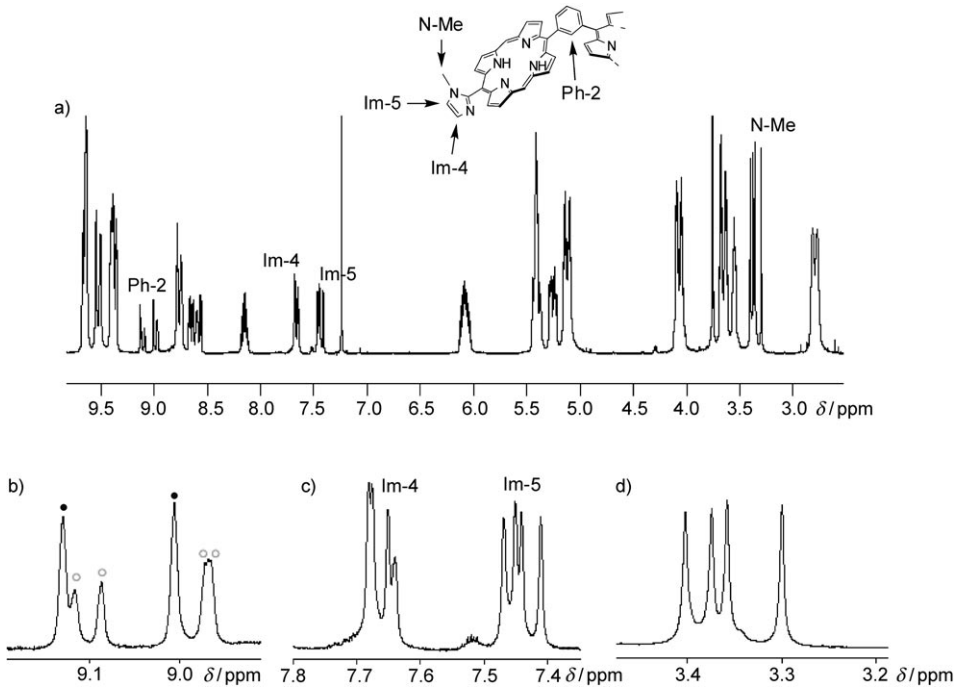

Figure 3. a) ^{1}H NMR spectrum of **1** in $CDCl_3$ at room temperature. Magnifications of the signals for Ph-2 (b), Im-4 and Im-5 (c), and Im N-Me (d) are also shown.

of 1:1. Further iodination of this mixture with bis(trifluoroacetoxy)iodobenzene (3 equiv) and I_2 (3 equiv) gave a mixture of **7** and tetraiodo-substituted **7** in a molar ratio of 1:1, which indicated that the iodination of *meta*-iodo-substituted phenyl occurred selectively. In this step, the use of an excess amount of bis(trifluoroacetoxy)-iodobenzene and I_2 is necessary because the *meta*-iodo-substituted compound cannot be removed even after the next coupling reaction. The coupling reaction of the mixture of **7** and tetraiodo-substituted **7** with 4-ethynylpyridine was carried out in the presence of $[Pd(PPh_3)_2Cl_2]$ and CuI.[20] Tetraiodo-substituted **7** was also coupled with 4-ethynylpyridine to afford the corresponding tetrapyridyl compound, which could be easily removed by means of silica gel column chromatography. The desired tripyridyl derivative **3** was isolated in a yield of 57% based on **7** as the starting mixture. The C_{60}–Tripod ligand was obtained in a yield of 21% by condensation of **3** with pyrrolidine–C_{60}[21] by using BOP as the coupling agent.

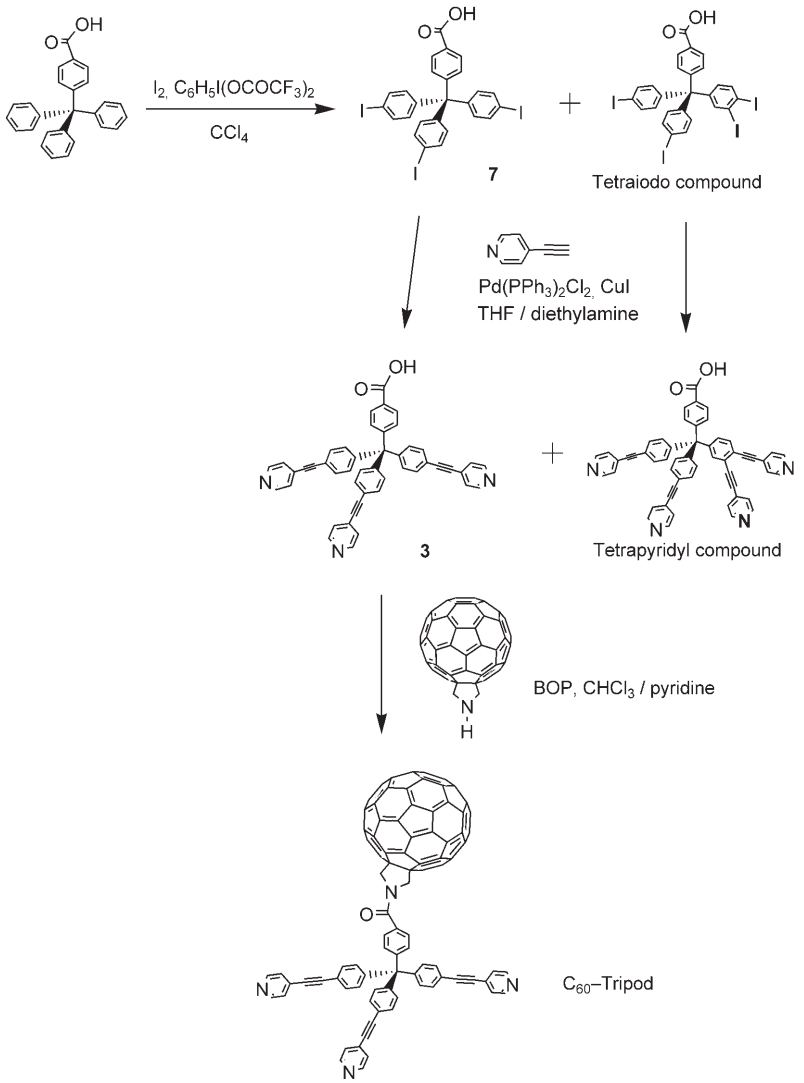

Scheme 2. Synthetic route of C_{60}–Tripod. BOP: 1*H*-benzotriazol-1-yloxytris-(dimethylamino)phosphonium hexafluorophosphate.

Reorganization of 1–Zn into a macrocycle: Treatment of **1** with $Zn(OAc)_2$ in $CHCl_3$ quantitatively afforded the corresponding zinc complex **1**–Zn (Scheme 3). During zinc insertion, insoluble material that resulted from a polymeric species of **1**–Zn was partially generated. This insoluble material was dissolved in $CHCl_3$, in which it was solubilized by the addition of a mixture of pyridine and toluene (1:2), and evaporated. This procedure converted the insoluble polymer into oligomeric assemblies of smaller molecular weights (Figure 4a). To convert the linear oligomers and any large ring compounds into macrocyclic species, the as-prepared mixture of **1**–Zn was subjected to a reorganization procedure in which a solution of the as-prepared mixture was diluted to 0.02 mM in $CHCl_3$/MeOH (9:1, v/v) and allowed to stand at 27 °C for one day in the dark. The solvent was carefully evaporated at 30 °C under reduced pressure.[22] The equilibrium of the complementary coordination of imidazolyl to zinc(II) under dilute conditions drives linear oligomers and larger ring compounds to converge into a single product that shows a sharp signal at 12.8 min in the gel permeation chromatogram (Figure 4b).[15] When the reorganization was performed under a higher methanol composition ($CHCl_3$/MeOH 7:3)[11c] or at lower temperature (≈17 °C), another assembly appeared at 12.3 min as a small signal in the gel permeation chromatogram (Figure 4b, inset). To obtain the single product appearing at 12.8 min, careful control of the solvent composition (methanol and chloroform) and temperature is required.

To determine the number of **1**–Zn units in the assembly, the MALDI-TOF mass spectrum of the assembly was measured. Even though the assembly was very stable in noncoordinating solvents, the assembled structure did not appear under the mass spectrometer conditions and predominantly showed a signal for monomeric **1**–Zn. To prevent the dissociation of the assembly under the mass spectrometer conditions, multisite ring-closing metathesis reactions[11c,18] of the *meso*-olefinic groups were carried out by using first-generation Grubbs catalyst.[23] The MALDI-TOF mass spectrum of the covalently linked assembly showed a signal corresponding to C-(**1**–Zn)$_3$ (calcd for [*M*+H]: *m*/*z*: 5816.5; found: 5816.4), which is the covalently linked trimer of **1**–Zn (Figure S1 in the Supporting Information). The coincidence between the theoretical and the observed molecular weights further supports the hypothesis that this assembly has no terminal olefinic groups, that is, it is the ring structure. The gel permeation chromatography (GPC) trace of C-(**1**–Zn)$_3$ also gave a sharp signal at a slightly longer retention time (12.9 min) than that of N-(**1**–Zn)$_3$, which reflects the loss of three ethylenic parts by the metathesis reaction (Figure S2 in the Supporting Information).

GPC analysis of the macrocycles and noncyclic oligomers: The GPC retention time gives information about the hydrodynamic volume, which reflects the molecular shape. To obtain further evidence for the ring structure of N-(**1**–Zn)$_3$, a series of noncyclic porphyrin arrays was prepared and

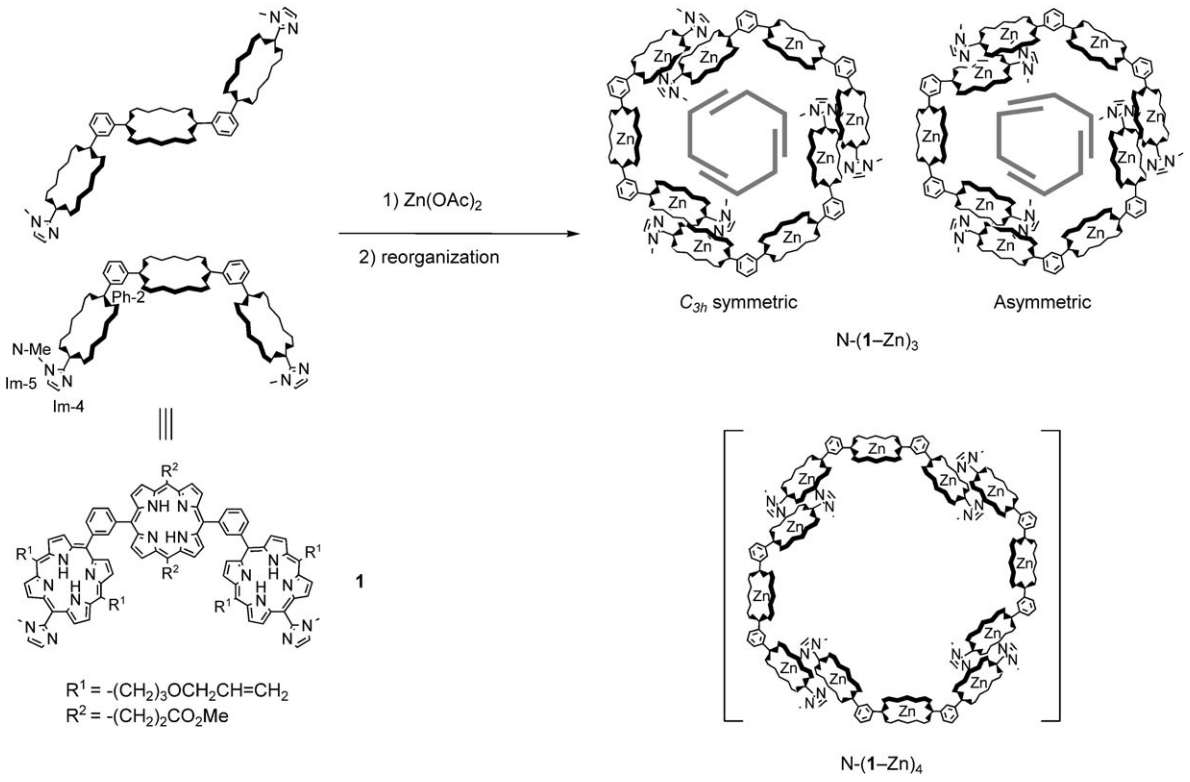

Scheme 3. Formation of the self-assembled macrocycle.

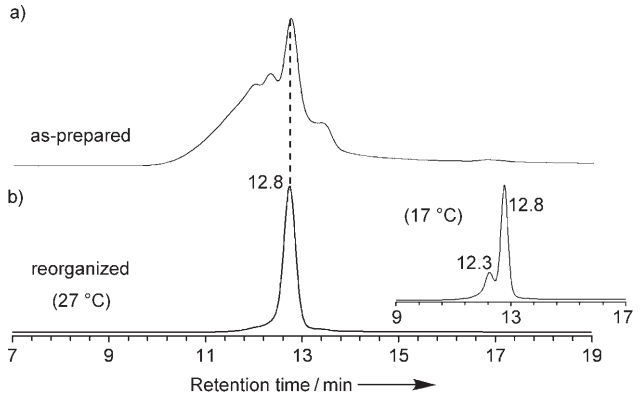

Figure 4. Gel permeation chromatograms of a) the as-prepared mixture and b) the reorganized sample of trisporphyrinatozinc(II) **1**–Zn treated with $CHCl_3$/MeOH = 9:1 and [**1**–Zn] = 0.02 mM at 27 °C. The inset shows the reorganized sample of **1**–Zn treated with $CHCl_3$/MeOH = 9:1 and [**1**–Zn] = 0.02 mM at 17 °C.

compared with the cyclic porphyrins by using GPC. Two types of noncyclic porphyrin arrays were prepared, array **9**, which has dimeric porphyrin units at both ends, and array **10**, which has monomeric units at the ends. They were prepared by mixing N-(**1**–Zn)$_3$ with N-(**5**–Zn)$_2$ or monoimidazolyl gable porphyrin **8**[14] in pyridine, followed by solvent evaporation. Dissolution of the residue in chloroform afforded a series of noncyclic porphyrin arrays (Scheme 4). The GPC charts of **9** and **10** are shown in Figure 5. Each signal in Figure 5a corresponds to noncyclic arrays **9** ($n = 0$, 1, 2, 3, and 4). Similarly, arrays **10** ($n = 0$, 1, and 2) were observed separately in Figure 5b. Figure 6 shows logarithmic plots of the molecular weights of the cyclic (●) and noncyclic (▲ and △) porphyrin arrays as a function of their retention times. The authentic cyclic gable pentamer and hexamer[11a,b] were also plotted (○). A dotted straight line was drawn connecting the open and filled triangles. Two series of the noncyclic arrays are on the straight line, which indicates that the hydrodynamic volume behaves similarly for different porphyrin ends. Cyclic arrays (N-(**1**–Zn)$_3$, its covalently linked derivative C-(**1**–Zn)$_3$, and the authentic gable pentamer and hexamer) are located above the line in an almost linear fashion. This result indicates that the cyclic arrays have smaller hydrodynamic volumes than the noncyclic arrays. The longer retention times observed for N-(**1**–Zn)$_3$ and C-(**1**–Zn)$_3$ compared with the noncyclic arrays (**9** and **10**) are fully consistent with the general tendency of the cyclic structures.[6g,24,25]

Structural analysis of the macrocycle by NMR spectroscopy: The unambiguous proof of the cyclic structure of N-(**1**–Zn)$_3$ was obtained by NMR spectroscopy analysis. Although the proton NMR spectrum of noncovalently linked cyclic trimer N-(**1**–Zn)$_3$ was complicated, most of the signals were assignable with support of 2D NMR measurements (COSY, TOCSY, and HMQC). COSY NMR spectroscopy showed that one set of four signals was correlated with another set of four signals (i.e., between $\delta = 4.55$–4.82 and 1.69–

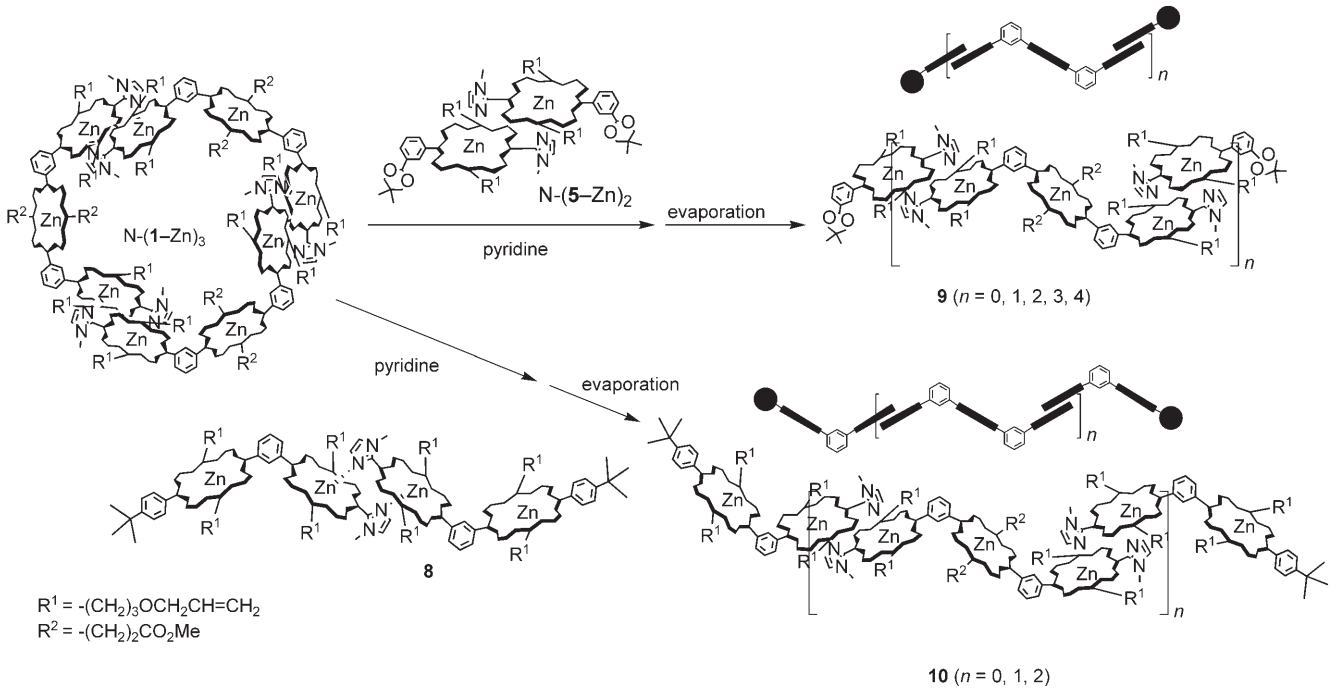

Scheme 4. Formation of the noncyclic porphyrin array.

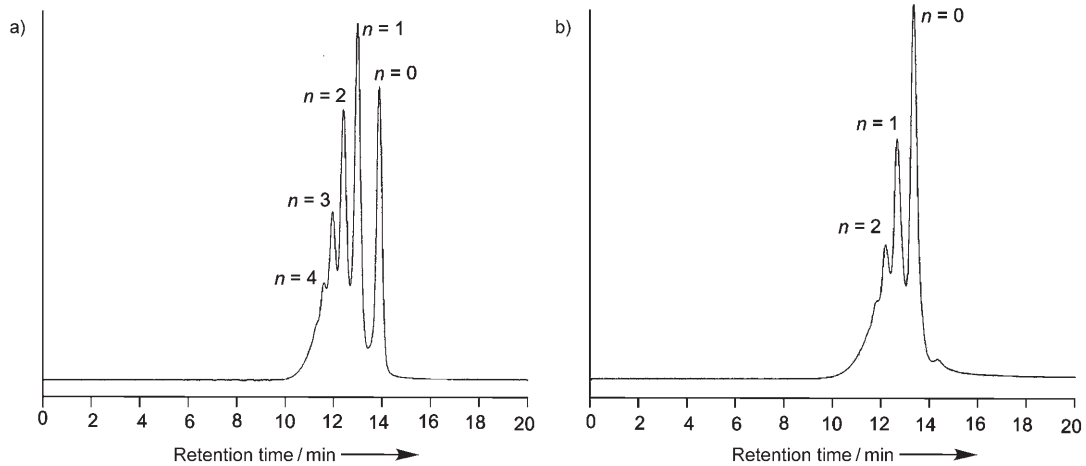

Figure 5. Gel permeation chromatograms of a series of noncyclic porphyrin arrays **9** (a) and **10** (b).

1.89 ppm, Figure 7) and HMQC (Figure S3 in the Supporting Information) showed that these signals were correlated with the signals of imidazolyl carbons ($\delta = \approx 120$ ppm). For all of the Im-4 and Im-5 protons, one set of four signals consisted of one big (○) and three small (●) signals with an integration ratio of 2:1, irrespective of "in" and "out" configurations (Figure 7). This signal integral ratio can be explained by assuming that there is a mixture of two topological isomers (C_{3h} symmetric[26] and asymmetric) in a ratio of 2:3. For each in and out proton, the signals of the C_{3h}-symmetric macrocycle exhibit only a single set of trisporphyrin signals because the three trisporphyrins are in the same environment. On the other hand, the signals of the asymmetric macrocycle show three sets of trisporphyrins because the three trisporphyrins are all in different environments. Thus, the one big (○) and three small (●) signals in Figure 7 can be assigned to the C_{3h}-symmetric and asymmetric macrocycles, respectively. The ratio (○/3●) corresponds to the formation ratio of the asymmetric and symmetric macrocycles.

The key signals that prove the cyclic structure are the imidazolyl protons inside and outside the ring. In the reference dimer, N-(**5**–Zn)$_2$, the Im-4 protons were observed at around 2.1 ppm because of the shielding effect of the coordinating porphyrin. For N-(**1**–Zn)$_3$, the Im-4 protons appeared in two different positions for the symmetric and asymmetric ring isomers. One of the groups of Im-4 protons

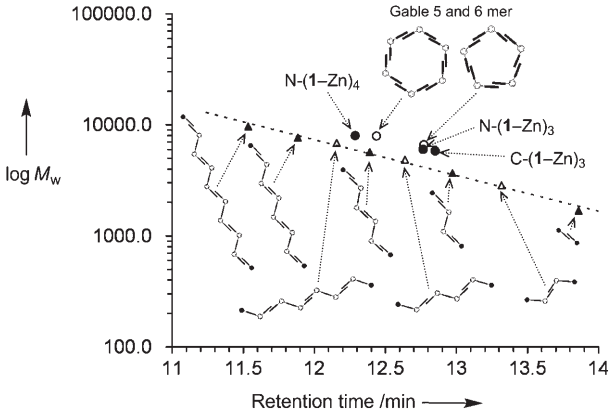

Figure 6. Plots of the retention time versus log M_w for cyclic and noncyclic porphyrin arrays. The dashed line is configured by a least-mean-squares approximation of the plots of noncyclic porphyrin arrays **9** (▲) and **10** (△). The hexameric and pentameric macrocycles of gable porphyrins[11a,b] are plotted as authentic samples of the cyclic structure.

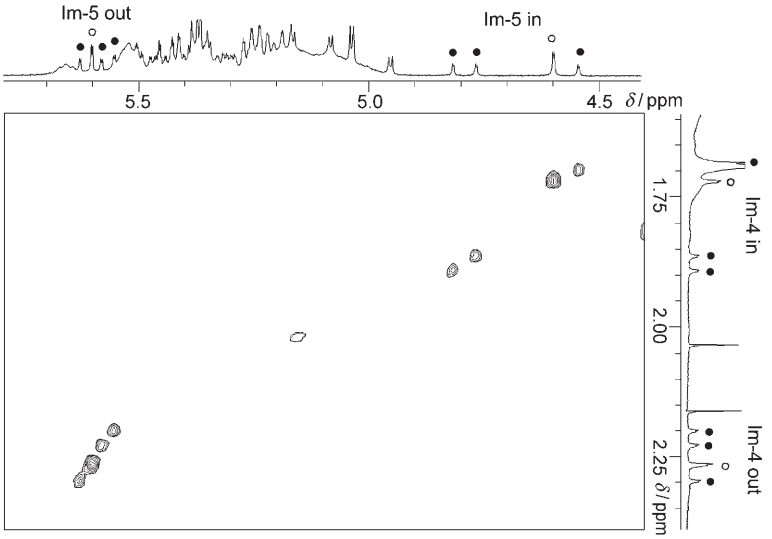

Figure 7. Correlation of the proton signals for Im-4 and Im-5 in N-(**1**–Zn)$_3$ on the COSY spectrum recorded at 600 MHz in $CDCl_3$.

appeared at $\delta = 2.26$ ppm in the C_{3h}-symmetric ring and at $\delta = 2.30$, 2.23, and 2.20 ppm in the asymmetric ring, and the other Im-4 protons appeared at $\delta = 1.72$ ppm in the C_{3h}-symmetric and $\delta = 1.89$, 1.86, and 1.69 ppm in the asymmetric rings. Whereas the former set of Im-4 protons was shifted to a similar position to that of N-(**5**–Zn)$_2$, the latter protons were further shifted to higher fields. Therefore, the former and latter signals can be assigned to the Im-4 protons outside and inside the ring, respectively. The inner protons should receive further upfield shifts of $\delta = 0.4$–0.5 ppm by anisotropic effects from other porphyrins of the ring components. A similar behavior was observed for the Im-5, N-Me, and β-pyrrole protons adjacent to the imidazolyl group.

Four signals for the inner Im-4 protons ranged over approximately 0.2 ppm ($\delta = 1.7$–1.9 ppm) in contrast to the outside protons, in which the range is approximately 0.1 ppm ($\delta = 2.2$–2.3 ppm; Figure 7). The larger shift range for the inner protons reflects the fact that the inner protons are influenced more strongly by the macrocycle topology. In addition, all of the outside N-Me protons of C_{3h}-symmetric and asymmetric macrocycles appeared at the same position ($\delta = 1.69$ ppm), which reflects the weak influences from the macrocycle topology. The difference in magnitude of the topological influence between inside and outside is also observed in the β-pyrrole proton adjacent to the imidazolyl group and the Im-5 protons.[15] The clear differentiation of these protons into a single signal or three different signals allows the assignment of the ring structures as C_{3h}-symmetric and asymmetric topological isomers, respectively.

Absorption and fluorescence properties of the macrocycle and complexation with a tetrapodal ligand: The absorption spectrum of macrocycle N-(**1**–Zn)$_3$ in toluene is shown in Figure 8 (solid line), and the peak positions of the Soret and Q bands are listed in Table 1. The Soret band exhibited a large split (at 411 and 443 nm; $\Delta E = 1760\ cm^{-1}$) by dipole–dipole exciton coupling[27] from slipped-cofacial and *m*-phenylene-bridged interactions. The shape of the Q band was close to the sum of N-(**5**–Zn)$_2$ and **6**–Zn in a ratio of 1:1, and a negligibly small excitonic coupling was observed (Figure S4 in the Supporting Information) because the Q bands of porphyrin have much smaller oscillator strengths than the Soret band.[28] The peaks at 565 and 619.5 nm correspond to the coordination dimer parts, whereas the peak at 556 nm is contributed from the uncoordinated

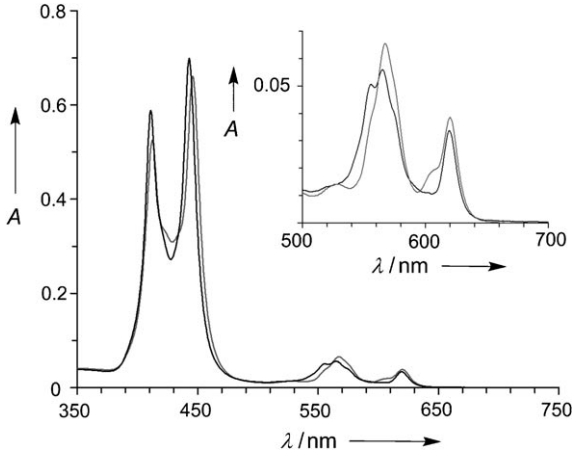

Figure 8. UV/Vis absorption spectra of N-(**1**–Zn)$_3$ (——) and N-(1Zn)$_3$ with of **2** (1.5 equiv; gray line) in toluene (5.6×10^{-7} M). The inset shows a magnification of the Q band region.

Table 1. Absorption and fluorescence spectral data in toluene.

	Absorption [nm]			Fluorescence[a] [nm]		Storks shift	ϕ_f[b]
	Soret	Q(1,0)	Q(0,0)	Q(0,0)	Q(0,1)	[cm^{-1}]	[%]
6–Zn	423	553	592	601	651	253	3.4
6–Zn/Im[c]	431	569	611	620	673	238	3.7
N-(**5**–Zn)$_2$	413.5, 437	566.5	618.5	622	681	91	4.9
N-(**1**–Zn)$_3$	411, 443	556, 565	619.5	623	680	91	5.1
N-(**1**–Zn)$_3$/**2**	412.5, 446	567	620	624	679	103	5.0

[a] Excited at 550 nm. [b] ϕ_f values were determined by using ZnTPP $\phi_f = 3.3\,\%$ as the standard value.[29,30] [c] In the presence of an excess amount of *N*-methylimidazole.

monomeric porphyrin units. The shift of the peak at 556 nm to a longer wavelength can be useful in monitoring coordination on the free porphyrinatozinc.

The steady-state fluorescence spectrum of N-(**1**–Zn)$_3$ was similar to that of dimer N-(**5**–Zn)$_2$ (Table 1). The fluorescence quantum yields (Φ_f) of monomer **6**–Zn, dimer N-(**5**–Zn)$_2$, and macrocycle N-(**1**–Zn)$_3$ were 3.4, 4.9, and 5.1 %, respectively. The quantum yield of N-(**5**–Zn)$_2$ is higher than that of **6**–Zn, and its Stokes shift is smaller (91 cm^{-1} for N-(**5**–Zn)$_2$ and 253 cm^{-1} for **6**–Zn), which indicates that the coordination dimer provides a more rigid structure and higher fluorescence intensity compared with **6**–Zn. The fluorescence quantum yield of N-(**1**–Zn)$_3$ was still maintained even though three monomeric porphyrins and three dimeric porphyrins were accumulated in close proximity. The high fluorescence quantum yield is favorable for the long-range excitation-energy transfer among the macrocycles by a singlet–singlet energy-transfer process.

We previously synthesized tetrapodal ligand **2** and studied its complexation with N-(**1**–Zn)$_3$. Judging from the CPK model[31] of the composite N-(**1**–Zn)$_3$/**2**, three pyridyl arms of **2** can adjust to fit the cavity of N-(**1**–Zn)$_3$ in both C_{3h}-symmetric and asymmetric isomers because of the flexibility of the carbon core that connects the four pyridyl arms. During a UV/Vis titration of **2** with N-(**1**–Zn)$_3$ in toluene, the Soret and Q bands were shifted towards longer wavelengths and the peak at 556 nm derived from the uncoordinated porphyrin disappeared.[15] This behavior indicates that **2** was accommodated in the ring of N-(**1**–Zn)$_3$ by three coordination bonds between pyridyl and zinc (Figure 8, gray line). The clear bending behavior observed at the point of [**2**]/[N-(**1**–Zn)$_3$] = 1 in the titration study and the Job plot[32] of the UV/Vis analysis also indicated the formation of a stable 1:1 complex between **2** and N-(**1**–Zn)$_3$ (Figure 1 and Figure S6 in ref. [15]). No heterogeneity of topological isomers was observed in these titrations. The binding constant was estimated to be $8\times10^8\,M^{-1}$ in toluene by curve-fitting analysis of the UV/Vis titration.[33] This large binding constant enables us to obtain the complex quantitatively under dilute conditions.[34] A ^{1}H NMR spectroscopy titration of **2** with N-(**1**–Zn)$_3$ was also performed in $CDCl_3$ ([N-(**1**–Zn)$_3$] = 2.6×10^{-4} M) to find the structure of the composite of **2** and N-(**1**–Zn)$_3$. However, the NMR spectra became very complex and broad upon the addition of **2** and it became difficult to assign the signals.

Complexation of the macrocycle with C_{60}–Tripod in benzonitrile: Photoinduced-electron-transfer experiments are usually conducted in polar solvents, such as benzonitrile, to stabilize the charge-separated state. Macrocycle N-(**1**–Zn)$_3$ is extremely, stable even in benzonitrile, as determined by the fact that the UV/Vis spectral shapes were unchanged in the concentration range of 10^{-6} to 10^{-8} M at 25 °C even after standing for several days. Therefore, it was not necessary to covalently connect the triporphyrin units by a metathesis reaction for the following photochemical measurements.

Table 2. Absorption and fluorescence spectral data in benzonitrile.

	Absorption [nm]			Fluorescence [nm]		ϕ_f[a]	Binding constant[b]
	Soret	Q(1,0)	Q(0,0)	Q(0,0)	Q(0,1)	[%]	[M^{-1}]
N-(**1**–Zn)$_3$	412.5, 445	565	619.5	624[c]	675[c]	3.9	–
N-(**1**–Zn)$_3$/**2**	413, 445	567	619.5	–	–	–	1.2×10^7
N-(**1**–Zn)$_3$/**3**	413, 445.5	567	619.5	624[d]	677[d]	3.9[e]	2.1×10^7
N-(**1**–Zn)$_3$/C_{60}–Tripod	414, 446	567	620	625[c]	676[c]	0.11[e]	3.1×10^8

[a] Fluorescence quantum yields were determined by using ZnTPP $\phi_f = 3.3\,\%$ as the standard value.[29,30] [b] Estimated from UV/Vis titration. [c] Excited at 427 nm. [d] Excited at 566 nm. [e] These values were calculated by assuming complexation of 100%.

The UV/Vis spectrum of N-(**1**–Zn)$_3$ in benzonitrile showed slight redshifts of the Soret and Q bands (Table 2) compared with those in toluene and disappearance of the peak at 556 nm, which indicated that benzonitrile is coordinated to the uncoordinated porphyrinatozinc(II) sites.[35] Titration of **2** with N-(**1**–Zn)$_3$ in benzonitrile showed that the Soret and Q bands were slightly redshifted with a decrease in the intensities. The binding constant was estimated to be $1.2\times10^7\,M^{-1}$ by curve fitting of the plot of change in absorbance at 444 nm as a function of the ratio of [**2**]/[N-(**1**–Zn)$_3$] (Figure S5 in the Supporting Information). Tripodal ligand **3**, which is the precursor for C_{60}–Tripod, was also titrated with N-(**1**–Zn)$_3$ in benzonitrile. The binding constant was estimated from the UV/Vis spectra to be $2.1\times10^7\,M^{-1}$. This value is of the same order of magnitude as that of **2**. The extremely high affinity of both **2** and **3**, even in the polar benzonitrile environment, must be achieved by three-point binding between pyridyl and zinc(II). Furthermore, the complexation of **3** did not affect the fluorescence of N-(**1**–Zn)$_3$

(Table 2), which indicated that the tripyridyl ligand moiety did not work as an acceptor for the excited energy of N-(**1**–Zn)$_3$.

Incorporation of C$_{60}$–Tripod into the ring of N-(**1**–Zn)$_3$ was examined by UV/Vis absorption and fluorescence titrations. The UV/Vis absorption spectral changes by complexation of C$_{60}$–Tripod with N-(**1**–Zn)$_3$ are shown in Figure 9. The Soret and Q bands were slightly redshifted with a decrease in intensities by the addition of C$_{60}$–Tripod. The fluorescence of N-(**1**–Zn)$_3$ was efficiently quenched by 85% with the addition of an equimolar amount of C$_{60}$–Tripod, and by 95% with four equivalents of C$_{60}$–Tripod (Figure 9).[36] The binding constant of C$_{60}$–Tripod to N-(**1**–Zn)$_3$ was estimated to be $3.1\times10^8\,\text{M}^{-1}$ from UV/Vis absorption and $3.4\times10^8\,\text{M}^{-1}$ from fluorescence titrations, respectively.[37] The value of $3\times10^8\,\text{M}^{-1}$ is approximately ten times larger than the values for tetrapodal ligand **2** and tripodal ligand **3** without the fullerene moiety, which suggests that the fullerene moiety significantly contributes to enhancing the binding of C$_{60}$–Tripod in N-(**1**–Zn)$_3$.

Time-resolved photophysical properties of the macrocycle and C$_{60}$–Tripod: To investigate the photophysical dynamics of the macrocycle/C$_{60}$–Tripod composite, time-resolved fluorescence decay and transient absorption were measured. Time-resolved fluorescence decay profiles of N-(**1**–Zn)$_3$ ([N-(**1**–Zn)$_3$]$=1.4\times10^{-6}$ M) in the absence and presence of C$_{60}$–Tripod (4 equiv) are shown in Figure S6 in the Supporting Information. Under these conditions, it is estimated that 99.92% of the macrocycle exists as the complex with C$_{60}$–Tripod. The fluorescence–time profile of N-(**1**–Zn)$_3$ decayed monoexponentially with a lifetime of 2100 ps, whereas that of the macrocycle/C$_{60}$–Tripod composite decayed biexponentially with time constants of 164 ps (62%) and 2100 ps (38%). A significant contribution of the longer lived component from free N-(**1**–Zn)$_3$ was observed. The quenching rate (k_q) and quantum yield (Φ_q) were evaluated to be $5.6\times10^9\,\text{s}^{-1}$ and 0.92% from the shorter τ_f component of the C$_{60}$–Tripod /N-(**1**–Zn)$_3$ composite according to Equations (1) and (2):

$$k_q = (1/\tau_f)_{\text{composite}} - (1/\tau_f)_{\text{macrocycle}} \quad (1)$$

$$\Phi_q = \frac{(1/\tau_f)_{\text{composite}} - (1/\tau_f)_{\text{macrocycle}}}{(1/\tau_f)_{\text{composite}}} \quad (2)$$

The quantum yield of the steady-state fluorescence quenching was estimated to be 0.97, which is compatible with the value of 0.92 calculated from the fluorescence decay when considering the errors associated with the respective measurements. The slow fluorescence decay was observed under the conditions in which complexation must be almost complete, which suggests that empty N-(**1**–Zn)$_3$ was regenerated under the high-laser-power conditions used for the lifetime measurements.

The nanosecond transient absorption spectra of N-(**1**–Zn)$_3$ in the absence and presence of C$_{60}$–Tripod in benzonitrile are shown in Figures S7 and S8 in the Supporting Information, respectively. The spectrum of N-(**1**–Zn)$_3$ after 50 μs (Figure S7) exhibited an absorption peak at 700 to 900 nm, which corresponded to the triplet excited state of zinc porphyrin. The nanosecond transient absorption spectra (Figure S8) of the complex between N-(**1**–Zn)$_3$ and C$_{60}$–Tripod did not show any clear peaks in the region from 700 to 1200 nm, which indicated that species from charge-separated and excited states were not detected on this timescale. To detect the short charge-separated state, picosecond transient absorption measurements of the complex were also examined in benzonitrile (Figure S9). However, the transient absorption spectra did not show apparent charge-separated species of either a porphyrin cation radical or a fullerene anion radical, but a broad and featureless absorption band was observed in the 600 to 800 nm region that extended over 1000 nm. The decay–time profile of the absorbance at 600 to 750 nm showed a lifetime of 77 ps ($k=1.3\times10^{10}\,\text{s}^{-1}$, Figure S10), which may correspond to the charge-recombination rate. Although the steady-state fluorescence and the time-resolved fluorescence decay indicated an efficient quenching of the singlet excited state of N-(**1**–Zn)$_3$, neither the nanosecond nor picosecond transient absorption spectra showed any detectable peaks of the radical ions, which suggested that the charge-recombination rate is as fast as the charge-separation rate.

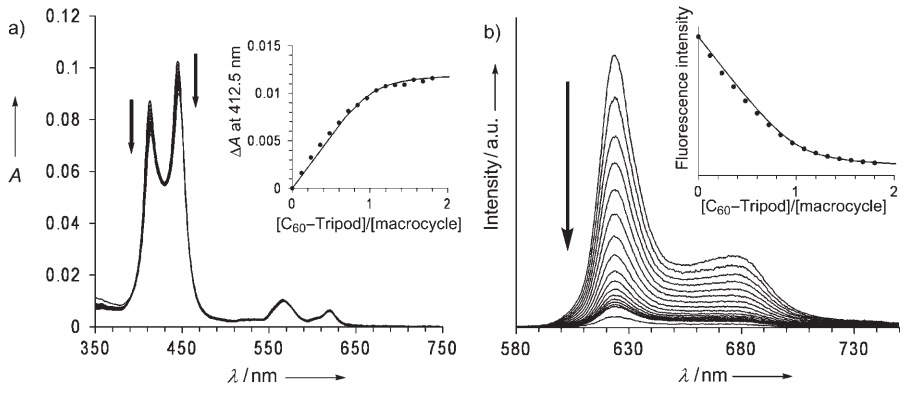

Figure 9. a) UV/Vis spectroscopy titration for the binding of N-(**1**–Zn)$_3$ with C$_{60}$–Tripod in benzonitrile. [N-(**1**–Zn)$_3$]$=7.2\times10^{-8}$ M, [C$_{60}$–Tripod]$=0$–1.8, 4 equiv, 25 °C. The inset shows the titration plot at 412.5 nm (●) and the theoretical curve for $K=3.1\times10^8\,\text{M}^{-1}$ (——). b) Steady-state fluorescence quenching of N-(**1**–Zn)$_3$ by C$_{60}$–Tripod in benzonitrile. Excited at 427 nm. [N-(**1**–Zn)$_3$]$=7.2\times10^{-8}$ M, [C$_{60}$–Tripod]$=0$–1.8, 4 equiv, 25 °C. The inset shows a plot of the change in the fluorescence intensity with the signal integration (580–750 nm; ●) and the theoretical curve for $K=3.4\times10^8\,\text{M}^{-1}$ (——).

Discussion

Atropisomers of 1: The ^{1}H NMR spectrum of **1** exhibited nonequivalent signals for imidazolyl and phenyl moieties (Figure 3). The number of the signals for the imidazolyl part (four) and the Ph-2 part (six) and their integration ratios are reasonably explained by considering the atropisomers (Figure 10): Two imidazolyl groups of **1** are separated at the terminal ends and the conformational differences at the opposite terminal imidazolyl group are negligible. Thus, the imidazolyl environments are affected by the relative conformation of N-Me to the central porphyrin (*Z* and *E*) and of the two terminal porphyrin planes (chair and boat), which results in four different environments (*Z* and *E* for the boat and chair conformers) for the imidazolyl group (Im-4, Im-5 and N-Me). In the case of the Ph-2 protons, their environments are affected by the two N-Me directions at both ends to afford six combinations of *ZZ*, *ZE* (=*EZ*), *EE* (1:2:1) of chair and boat conformers. Although **1** has several atropisomers as a result of their slow exchange rate on the NMR timescale, isomerizations among atropisomers took place under reorganization conditions in the ring-forming procedure.[11b]

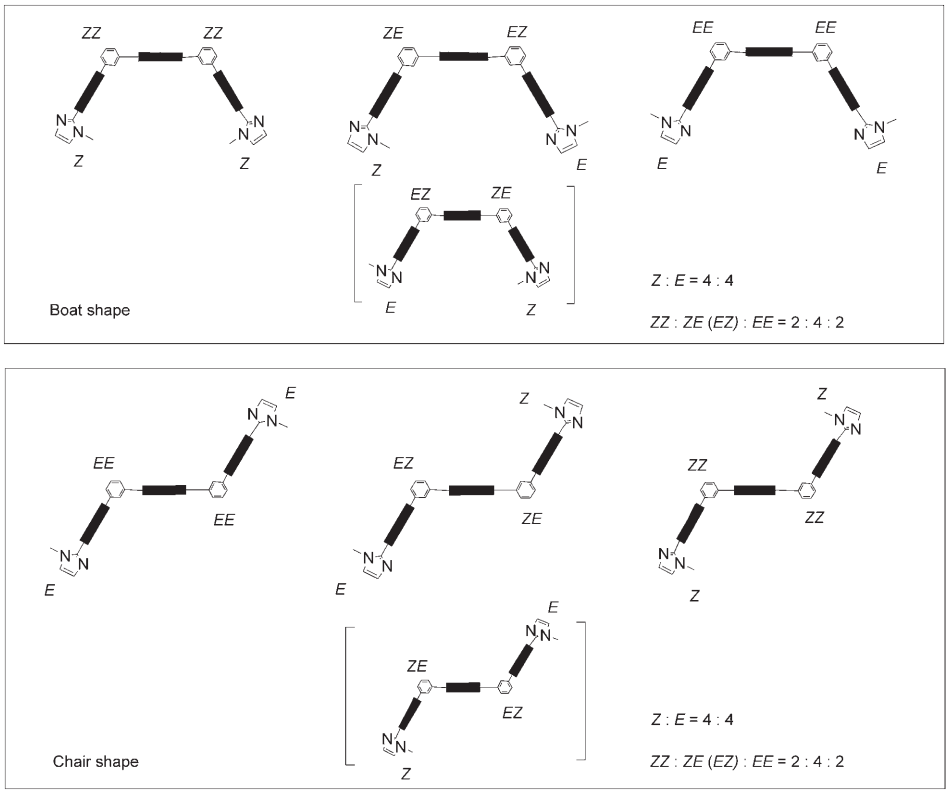

Figure 10. Schematic structure of atropisomers in **1**. The isomers *ZZ*, *ZE* (*EZ*), and *EE* were named according to the conformation of the imidazolyl moiety (*Z* and *E*).

Selective formation of the macrocycle: The coordination of imidazolyl to zinc(II) in imidazolyl-substituted porphyrins affords an ideal complementarity to form a dimer with a binding constant that reaches $10^{11}\,\text{M}^{-1}$ in toluene. Even though the dimer is stabilized by complementary coordination coupled with π–π interactions in nonpolar solvents, the structure can be easily dissociated into the monomer by adding coordinating solvents, such as MeOH or pyridine. The combination of formation and dissociation enables us to construct macrocyclic structures by a reorganization process.

Because zinc insertion into **1** was performed at a relatively high concentration ([**1**] = 1.44 mM),[15] self-assembled polymers of **1**–Zn were formed along with cyclic species. To eliminate the polymers, we applied the reorganization process by using a mixed solvent of $CHCl_3$/MeOH (9:1, v/v) and a low concentration ([**1**–Zn] = 0.02 mM). Formation of polymers is entropically unfavorable, and the polymers turn into smaller molecular species under dilute conditions. In addition, the cyclic structures satisfy all of the complementary coordinations of imidazolyl to zinc and are enthalpically favorable. Combined factors drive small oligomers into cyclic structures. When the reorganization process was performed at a relatively low temperature (≈17 °C), GPC analysis showed a small signal at 12.3 min along with a major signal for N-(**1**–Zn)$_3$ (Figure 4b, inset). The signal at 12.3 min is assigned as the cyclic tetramer of **1**–Zn (N-(**1**–Zn)$_4$).[38] When a higher temperature (27 °C) was used in the reorganization process, formation of N-(**1**–Zn)$_4$ was suppressed and cyclic trimer N-(**1**–Zn)$_3$ was formed exclusively. Negative enthalpy and entropy changes (ΔH and ΔS) are expected on formation of macrocycles from **1**–Zn. Because the larger cyclic oligomers presumably have a more negative ΔS than the smaller macrocycles, the smaller rings are preferentially obtained, which was demonstrated in the case of ferrocene-bridged trisporphyrin.[25] It is the same reason that a higher temperature makes the formation of N-(**1**–Zn)$_4$ unfavorable by the more negative entropy term ($-T\Delta S$) than that of N-(**1**–Zn)$_3$. In this case, the formation of a cyclic dimer was not observed because of unfavorable strain energies.

Cyclic trimer N-(**1**–Zn)$_3$ possesses two topological isomers, C_{3h} symmetric and asymmetric, in a ratio of 2:3. The statistical distribution should give a ratio of 1:3 for the C_{3h}-symmetric and asymmetric isomers, which means that the

C_{3h}-symmetric isomer is favored by a factor of two. Of course, the C_{3h}-symmetric isomer is free from angle strain for the formation of the cyclic trimer. Because these isomers behave similarly when accommodating tetrapodal and tripodal ligands, the structural heterogeneity of the isomers does not seem to produce any problems.

Complexation of the tripodal ligand with the macrocycle: We previously reported that a slipped-cofacial dimer attached to a fullerene afforded a stable charge-separated state by photoexcitation of the porphyrins.[39] Because the first one-electron oxidation potential of pyridine-coordinated porphyrinatozinc is similar to that of the complementary coordination dimer[40] and the energy gap between the ground and the lowest excited states is also almost the same,[41] both of the excited porphyrin units in the composite of N-(**1**–Zn)$_3$ and C_{60}–Tripod are considered to have a similar ability for electron donation. Thus, the fullerene unit in C_{60}–Tripod can accept an electron from all of the porphyrin components in the ring. The center-to-center distance from each porphyrin in N-(**1**–Zn)$_3$ to the fullerene moiety of C_{60}–Tripod in the complex is estimated to be 15 to 20 Å by assuming three-point coordination from the tripodal pyridyl ligands to the uncoordinated porphyrinatozinc(II) sites (Figure 11a). Judging from this distance (15–20 Å), we reasonably expected that the complex of N-(**1**–Zn)$_3$ and C_{60}–Tripod would have a long lifetime for the charge-separated state by photoexcitation of the porphyrins in N-(**1**–Zn)$_3$. Efficient fluorescence quenching of N-(**1**–Zn)$_3$ observed in the steady-state fluorescence titration studies clearly showed that fast electron transfer from the excited porphyrin to the fullerene occurred in the complex in which all of the porphyrin pairs act as one fluorescence chromophore. However, the transient absorption spectra of nano- and picosecond timescales were featureless, which showed that there was no definitive charge-separated species nor any triplet excited state of either porphyrin or fullerene. This strongly indicates that fast charge recombination to the ground state occurs after the initial charge separation, which suggests that the fullerene and the porphyrin are closely positioned in the macrocycle.

The binding constant of C_{60}–Tripod to N-(**1**–Zn)$_3$ in benzonitrile was determined to be $3\times10^8\,\text{M}^{-1}$, which was approximately ten times larger than the values for tetrapodal ligand **2** and tripodal ligand **3** without the fullerene moiety (Table 2). This larger binding constant indicates that the binding mode of C_{60}–Tripod to N-(**1**–Zn)$_3$ is different from that expected for three-point coordination from pyridyls to uncoordinated porphyrinatozinc sites. These results suggest that the fullerene moiety in C_{60}–Tripod has fallen down into the inner surface of N-(**1**–Zn)$_3$ to make direct contact between the fullerene and the porphyrin through π–π interactions,[42] which is a structure that is acceptable according to the CPK model (Figure 11b). In this conformation the fullerene moiety of C_{60}–Tripod is in direct contact with and strongly interacts with one or two porphyrins of N-(**1**–Zn)$_3$. Actually, Hirsch et al. reported porphyrinatozinc(II)–fullerene π-stacked dyads, which formed the charge-transfer state by strong π–π interactions.[43,44] Their transient absorption spectra showed broad and featureless absorption bands in the wide range of 600 to 1000 nm with a decay time of 38 ps in benzonitrile, which is attributed to the exciplex[43a] and is comparable to the lifetime (77 ps) of the charge-separated state or exciplex of N-(**1**–Zn)$_3$ and C_{60}–Tripod. Furthermore, the fluorescence quenching rate of N-(**1**–Zn)$_3$ by C_{60}–Tripod does not appreciably change in toluene and benzonitrile. This would be compatible with the explanation that charge separation occurs without bridging solvent molecules, that is, through a direct pathway between the porphyrin and the fullerene.[43a]

We have reported that the excitation energy hopping times through *m*-phenylene linkages were 8.0 and 5.3 ps in pentameric and hexameric macrocycles of gable porphyrin, respectively.[14] In the complex of N-(**1**–Zn)$_3$ and C_{60}–Tripod, comparable energy hopping times are expected because the coordinated monomeric porphyrin has a similar excited energy level to that of the dimeric porphyrin. Actually, on complexation of C_{60}–Tripod, the fluorescence of N-(**1**–Zn)$_3$ from both monomeric and dimeric porphyrin units was completely quenched, which demonstrated that the excitation energy migrates rapidly among the porphyrins and then converges on the fullerene moiety by electron transfer.

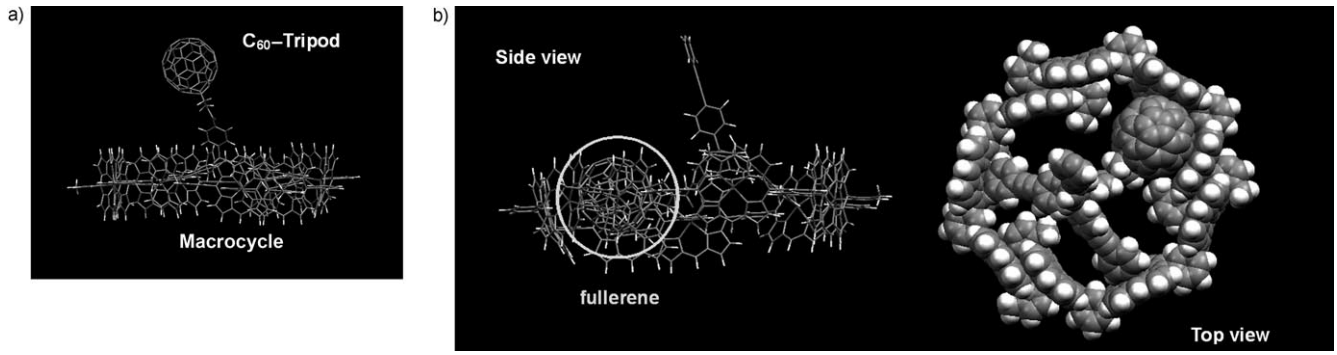

Figure 11. The CPK model of C_{60}–Tripod /N-(**1**–Zn)$_3$, which was created by using Cerius^2 software,[31] based on a) three pyridyl coordinations and b) two pyridyl coordination and fullerene–porphyrin π–π interactions.

Conclusion

Cyclic trimer N-(**1**–Zn)$_3$ could be obtained exclusively from trisporphyrinatozinc(II) **1**–Zn appended with imidazolyl groups at the terminal porphyrins when the appropriate conditions were applied in the reorganization process. Macrocycle N-(**1**–Zn)$_3$ accommodated tripodal ligands with two kinds of binding modes. Model ligand **2** and the tripodal ligand without fullerene (**3**) were bound by using three-point coordinations from the pyridyl ligands to uncoordinated porphyrinatozinc(II) sites of N-(**1**–Zn)$_3$, the binding constants of which are estimated to be $1–2\times10^7\,\text{M}^{-1}$ in benzonitrile. The fullerene–tripodal ligand (C_{60}–Tripod) was bound by using two-point coordinations from the pyridyl ligands to uncoordinated porphyrinatozinc(II) sites of N-(**1**–Zn)$_3$ and fullerene–porphyrin π–π interactions, the binding constant of which was estimated to be $3\times10^8\,\text{M}^{-1}$ in benzonitrile. Direct contact of the fullerene moiety to porphyrin produced a binding constant ten times larger than the values for three-point coordinations, and complete quenching of the fluorescence of N-(**1**–Zn)$_3$. The large binding constant enabled us to quantitatively obtain the complex of C_{60}–Tripod with N-(**1**–Zn)$_3$ by the addition of equivalent tripodal ligands under dilute conditions ($\approx10^{-6}$ M) even in benzonitrile, and to utilize C_{60}–Tripod as a fluorescence quencher for investigations into the energy-transfer process among the macrocycles. Because displacement of the fourth arm of the tripodal ligand is easily achieved, the present method is applicable for introducing various types of functional groups, and to construct their composites with porphyrin macrocycles.

Experimental Section

General procedure: The syntheses of porphyrins **1**, N-(**1**–Zn)$_3$, C-(**1**Zn)$_3$, **2**, **4**, **5**, N-(**5**–Zn)$_2$, **6**, and **6**–Zn have been previously reported.[15] All chemicals and solvents were of commercial reagent quality, and used without further purification unless otherwise stated. Dry THF was prepared by distillation over benzophenone-Na. Dry DMF, Et_2NH, and Et_3N were prepared by distillation over CaH_2. First generation Grubbs catalyst (benzylidene-bis(tricyclohexylphosphine)dichlororuthenium) was purchased from Aldrich. ^{1}H NMR spectra were recorded by using a JEOL ECP-600 (600 MHz) spectrometer and chemical shifts were recorded in parts per million (ppm) relative to tetramethylsilane. UV/Vis absorption spectra were recorded by using a Shimadzu UV-3100PC spectrometer. Steady-state fluorescence emission spectra were recorded by using a Hitachi F-4500 spectrometer and corrected for the response of the detector system. The fluorescence intensities were normalized at the absorption of their excitation wavelength. UV/Vis λ_{max} values are reported in nm. Fluorescence quantum yields were determined by corrected integrated ratios of steady-state fluorescence spectra relative to that of tetraphenylporphyrinatozinc (ZnTPP; $\Phi_f=3.3\,\%$).[29] UV/Vis and fluorescence titrations were performed by adding a solution of pyridyl ligand to a solution of N-(**1**–Zn)$_3$ in a quartz cuvette (1 cm path length) by using microliter syringes. MALDI-TOF mass spectra were obtained by using a PerSeptive Biosystems Voyager DE-STR instrument with dithranol (Aldrich) as the matrix. Analytical gel permeation chromatograms were obtained by using a Hewlett Packard HP1100 series instrument equipped with an analytical JAIGEL 3HA column (Japan Analytical Industry, 8 mm × 500 mm, exclusion limit = 70,000 Da). Reactions were monitored on silica gel 60 F_{254} TLC plates (Merck). The silica gel utilized for column chromatography was purchased from Kanto Chemical (Silica Gel 60N (Spherical, Neutral) 60–210 μm).

4-Tris(4-iodophenyl)methylbenzoic acid 7: 4-(Tripenylmethyl)benzoic acid[19] (123 mg, 3.18×10^{-4} mol), bis(trifluoroacetoxy)iodobenzene (684 mg, 1.59×10^{-3} mol) and iodine (404 mg, 1.59×10^{-3} mol) were dissolved in CCl_4 (3 mL). The mixture was stirred for 3 h at 60 °C. After the mixture was cooled to room temperature, the reaction mixture was diluted with $CHCl_3$ (≈50 mL), and then washed successively with aqueous sodium bisulfite and water. The organic layer was evaporated to dryness and the residue was purified by means of a short column (SiO_2: $CHCl_3$ to $CHCl_3$/MeOH 9:1). The invisible second fraction, which eluted with 10 % MeOH/$CHCl_3$, was collected and evaporated to afford a pale yellow solid (234 mg). The integral values of ^{1}H NMR signals indicated that the solid was a mixture of **7** (108 mg, 46 %) and tetraiodo-substituted **7** (126 mg) in a molar ratio of 1:1. *7*: ^{1}H NMR (600 MHz, $CDCl_3$): $\delta=7.98$ (d, $J=8.5$ Hz, 2H; Ph′), 7.61 (d, $J=8.8$ Hz, 6H; Ph), 7.28 (d, $J=8.5$ Hz, 2H; Ph′), 6.89 (d, $J=8.8$ Hz, 6H; Ph). Tetraiodo-substituted **7**: ^{1}H NMR (600 MHz, $CDCl_3$): $\delta=8.00$ (d, $J=8.2$ Hz, 2H; Ph′), 7.74 (d, $J=8.5$ Hz, 1H; Ph-5), 7.67, (d, $J=2.2$ Hz, 1H; Ph-2), 7.60 (d, $J=8.8$ Hz, 4H; Ph), 7.26–7.27 (d, 2H; Ph′), 6.90 (d, $J=8.8$ Hz, 4H; Ph), 6.81 ppm (dd, $J=8.5$, 2.2 Hz, 1H; Ph-6).

4-Tris[4-{2-(4-pyridyl)ethynyl}phenyl]methylbenzoic acid 3: 4-Tris(4-iodophenyl)methylbenzoic acid (32 mg, 4.3×10^{-5} mol, the amount of tetraiodo-substituted **7** (38 mg) was subtracted from 70 mg of the impure sample), 4-ethynylpyridine[45] (40 mg, 3.9×10^{-4} mol), $Pd(PPh_3)_2Cl_2$ (13 mg, 1.9×10^{-5} mol), CuI (4 mg, 1.9×10^{-5} mol), dry Et_2NH (0.5 mL), and dry THF (0.5 mL) were placed in a Schlenk flask under an argon atmosphere. The mixture was degassed by freeze–thaw cycles and stirred for 12 h at room temperature under argon. The reaction mixture was diluted with $CHCl_3$ and washed with saturated aqueous NaCl and water. The solvent was evaporated and the residue was purified by means of column chromatography (SiO_2; $CHCl_3$/MeOH 99:1 to 93:7). The third fraction was collected and evaporated to afford **3** (16.5 mg, 57 %). ^{1}H NMR (600 MHz, $CDCl_3$): $\delta=8.62$ (d, $J=5.9$ Hz, 6H; Py), 8.03 (d, $J=$ 8.2 Hz, 2H; Ph′), 7.49 (d, $J=8.2$ Hz, 6H; Ph), 7.39 (d, $J=5.9$ Hz, 6H; Py), 7.33 (d, $J=8.2$ Hz, 2H; Ph′), 7.25 (d. $J=8.2$ Hz, 6H; Ph), 1.94 ppm (br s; COOH); MALDI-TOF: m/z: 668.0 [M+H].

C_{60}–Tripod: 4-Tris[4-{2-(4-pyridyl)ethynyl}phenyl]methylbenzoic acid (11 mg, 1.7×10^{-5} mol) and BOP (7 mg, 1.7×10^{-5} mol) were placed in a 20 mL flask and purged with argon gas. $CHCl_3$ (2.5 mL) and pyridine (0.5 mL) were added to the mixture, and the mixture was stirred for 10 min at room temperature. Pyrrolidine–C_{60} TFA salt[21] (13 mg, 1.5×10^{-5} mol) was then added and the reaction mixture was stirred at room temperature. The reaction progress was monitored by MALDI-TOF mass spectrometry. After stirring for 24 h, further BOP (14 mg, 3.2×10^{-5} mol) was added to the reaction mixture to promote the reaction, and stirring was continued for another 24 h. The solvent was evaporated to give a crude residue. The residue was purified with by column chromatography (SiO_2; $CHCl_3$/MeOH 95:5) and the brown band was collected. This fraction was evaporated and further reprecipitated with hexane to give C_{60}–Tripod as a brown solid (4.8 mg, 21 %): $R_f=0.6$ (SiO_2; $CHCl_3$/MeOH 9:1); ^{1}H NMR (600 MHz, $CDCl_3$): $\delta=8.61$ (br s, 6H; Py), 7.85 (d, $J=$ 8.5 Hz, 2H; Ph′), 7.51 (d, $J=8.5$ Hz, 6H; Ph), 7.46 (d, $J=8.5$ Hz, 2H; Ph′), 7.37 (br d, $J=4.9$ Hz, 6H; Py), 7.30 (d, $J=8.5$ Hz, 6H; Ph), 5.56 ppm (br s, CH_2); ^{13}C NMR (150 MHz, $CDCl_3$): $\delta=169.8$, 149.8, 148.6, 147.4, 146.43, 146.40, 146.2, 145.6, 145.53, 145.45, 145.40, 144.5, 143.2, 143.1, 142.8, 142.2, 142.1, 142.0, 140.2, 133.2, 131.6, 131.3, 131.2, 131.0, 128.1, 125.5, 120.6, 93.3, 87.3 ppm; UV/Vis ($CHCl_3$): λ_{max} (ε): 432 (2900), 698.5 nm (290 $\text{mol}^{-1}\,\text{dm}^3\,\text{cm}^{-1}$); MALDI-TOF: m/z: 1414.0 [M+H].

Noncyclic porphyrin array 9 (10): Pyridine (0.5 mL) was added to a mixture of N-(**1**–Zn)$_3$ (1.2 mg, 2.0×10^{-7} mol) and N-(**5**–Zn)$_2$ (1.0 mg, 6.0×10^{-7} mol) in $CHCl_3$ (10 mL), and then the solvents were evaporated to dryness under reduced pressure. The residue was dissolved in $CHCl_3$ and subjected to GPC analysis. The preparation of series **10** were performed with the same procedure as that used for **9** except **8** was used instead of N-(**5**–Zn)$_2$.

Time-resolved emission and transient absorption measurements: The fluorescence lifetimes were measured by using an argon-ion pumped Ti/sapphire laser (Tsunami) and a streak scope (Hamamatsu Photonics). The nanosecond transient absorption spectra in the NIR region were measured by means of laser-flash photolysis; 565 nm light from Nd/YAG laser was used as the exciting source, and a Ge-avalanche-photodiode module was used for detecting the monitoring light from a pulsed Xe lamp. The picosecond transient absorption spectra were measured by the pump and probe method by using a Ti/sapphire regenerative amplifier seeded by the SHG of an Er-doped fiber laser (Clark-MXR CPA-2001 plus). The details of the experimental setup are described elsewhere.[46]

Acknowledgements

This work was supported by Grants-in-Aid for Scientific Research (A) (Y.K.) from the Japan Society for the Promotion of Science (JSPS).

[1] R. E. Blankenship, *Molecular Mechanisms of Photosynthesis*, Blackwell Science, Oxford, **2002**.

[2] a) S. Karrasch, P. A. Bullough, R. Ghosh, *EMBO J.* **1995**, *14*, 631; b) A. W. Roszak, T. D. Howard, J. Southall, A. T. Gardiner, C. L. Law, N. W. Isaacs, R. J. Cogdell, *Science* **2003**, *302*, 1969.

[3] a) G. McDermott, S. M. Prince, A. A. Freer, A. M. Hawthornthwaite-Lawless, M. Z. Papiz, R. J. Cogdell, N. W. Isaacs, *Nature* **1995**, *374*, 517; b) J. Koepke, X. Hu, C. Muenke, K. Schulten, K. Michel, *Structure* **1996**, *4*, 581.

[4] a) S. Bahatyrova, R. N. Frese, C. A. Siebert, J. D. Olsen, K. O. van der Werf, R. van Grondelle, R. A. Niederman, P. A. Bullough, C. Otto, C. N. Hunter, *Nature* **2004**, *430*, 1058; b) S. Scheuring, J. N. Sturgis, V. Prima, A. Bernadac, D. Levy, J.-L. Rigaud, *Proc. Natl. Acad. Sci. USA* **2004**, *101*, 11293; c) S. Scheuring, J. N. Sturgis, *Science* **2005**, *309*, 484.

[5] For recent reviews, see: a) J. K. M. Sanders in *Comprehensive Supramolecular Chemistry, Vol. 9* (Eds.: J. L. Atwood, J. E. D. Davies, D. D. MacNicol, F. Vögtle), Pergamon, Oxford, **1996**, pp. 131; b) J. Chambron, V. Heitz, J. P. Sauvage in *The Porphyrin Handbook, Vol. 6* (Eds.: K. M. Kadish, K. M. Smith, R. Guilard), Academic Press, New York, **2000**, pp. 1; c) A. K. Burrell, D. L. Officer, P. G. Plieger, D. C. W. Reid, *Chem. Rev.* **2001**, *101*, 2751; d) P. D. Harvey in *The Porphyrin Handbook, Vol. 18* (Eds.: K. M. Kadish, K. M. Smith, R. Guilard), Academic Press, New York, **2003**, pp. 63; e) M.-S. Choi, T. Yamazaki, I. Yamazaki, T. Aida, *Angew. Chem.* **2004**, *116*, 152; *Angew. Chem. Int. Ed.* **2004**, *43*, 150; f) Y. Kobuke, *Eur. J. Inorg. Chem.* **2006**, 2333; g) Y. Nakamura, N. Aratani, A. Osuka, *Chem. Soc. Rev.* **2007**, *36*, 831.

[6] For recent reports of covalent linking cyclic array, see: a) S. Anderson, H. L. Anderson, A. Bashall, M. McPartlin, J. K. M. Sanders, *Angew. Chem.* **1995**, *107*, 1196; *Angew. Chem. Int. Ed. Engl.* **1995**, *34*, 1096; b) H. A. M. Biemans, A. E. Rowan, A. Verhoeven, P. Vanoppen, L. Latterini, J. Foekema, A. P. H. J. Schenning, E. W. Meijer, F. C. de Schryver, R. J. M. Nolte, *J. Am. Chem. Soc.* **1998**, *120*, 11054; c) J. Li, A. Ambroise, S. I. Yang, J. R. Diers, J. Seth, C. R. Wack, D. F. Bocian, D. Holten, J. S. Lindsey, *J. Am. Chem. Soc.* **1999**, *121*, 8927; d) O. Mongin, A. Schuwey, M.-A. Vallot, A. Gossauer, *Tetrahedron Lett.* **1999**, *40*, 8347; e) O. Mongin, N. Hoyler, A. Gossauer, *Eur. J. Org. Chem.* **2000**, 1193; f) M. Takase, R. Ismael, R. Murakami, M. Ikeda, D. Kim, H. Shinmori, H. Furuta, A. Osuka, *Tetrahedron Lett.* **2002**, *43*, 5157; g) X. Peng, N. Aratani, A. Takagi, T. Matsumoto, T. Kawai, L.-W. Hwang, T. K. Ahn, D. Kim, A. Osuka, *J. Am. Chem. Soc.* **2004**, *126*, 4468; h) M. C. Lensen, S. J. T. van Dingenen, J. A. A. W. Elemans, H. P. Dijkstra, G. P. M. van Klink, G. van Koten, J. W. Gerritsen, S. Speller, R. J. M. Nolte, A. E. Rowan, *Chem. Commun.* **2004**, 762; i) A. Kato, K. Sugiura, H. Miyasaka, H. Tanaka, T. Kawai, M. Sugimoto, M. Yamashita, *Chem. Lett.* **2004**, *33*, 578; j) Y. Nakamura, L.-W. Hwang, N. Aratani, T. K. Ahn, D. M. Ko, A. Takagi, T. Kawai, T. Matsumoto, D. Kim, A. Osuka, *J. Am. Chem. Soc.* **2005**, *127*, 236; k) M. Hoffmann, C. J. Wilson, B. Odell, H. L. Anderson, *Angew. Chem.* **2007**, *119*, 1; *Angew. Chem. Int. Ed.* **2007**, *46*, 3122.

[7] For recent reports of noncovalently linked cyclic array, see: a) C. M. Drain, K. C. Russell, J.-M. Lehn, *Chem. Commun.* **1996**, 337; b) S. Knapp, J. Vasudevan, T. J. Emge, B. H. Arison, J. A. Potenza, H. J. Schugar, *Angew. Chem.* **1998**, *110*, 2537; *Angew. Chem. Int. Ed.* **1998**, *37*, 2368; c) C. Ikeda, N. Nagahara, E. Motegi, N. Yoshioka, H. Inoue, *Chem. Commun.* **1999**, 1759; d) R. A. Haycock, A. Yartsev, U. Michelsen, V. Sundström, C. A. Hunter, *Angew. Chem.* **2000**, *112*, 3762; *Angew. Chem. Int. Ed.* **2000**, *39*, 3616; e) R. A. Haycock, C. A. Hunter, D. A. James, U. Michelsen, L. R. Sutton, *Org. Lett.* **2000**, *2*, 2435; f) A. Tsuda, T. Nakamura, S. Sakamoto, K. Yamaguchi, A. Osuka, *Angew. Chem.* **2002**, *114*, 2941; *Angew. Chem. Int. Ed.* **2002**, *41*, 2817; g) T. Kamada, N. Aratani, T. Ikeda, N. Shibata, Y. Higuchi, A. Wakamiya, S. Yamaguchi, K.-S. Kim, Z.-S. Yoon, D. Kim, A. Osuka, *J. Am. Chem. Soc.* **2006**, *128*, 7670.

[8] D. M. Guldi, M. Prato, *Acc. Chem. Res.* **2000**, *33*, 695.

[9] For reviews of covalently linked porphyrin and fullerene conjugates, see: a) D. Gust, T. A. Moore in *The Porphyrin Handbook, Vol. 8*, (Eds.: K. M. Kadish, K. M. Smith, R. Guilard), Academic Press, New York, **2000**, pp. 153; b) H. Imahori, *Org. Biomol. Chem.* **2004**, *2*, 1425.

[10] For reports of a noncovalently linked porphyrin and fullerene conjugate, see: a) N. Armaroli, F. Diederich, L. Echegoyen, T. Habicher, L. Flamigni, G. Marconi, J.-F. Nierengarten, *New J. Chem.* **1999**, *23*, 77; b) F. D'Souza, G. R. Deviprasad, M. S. Rahman, J.-P. Choi, *Inorg. Chem.* **1999**, *38*, 2157; c) T. Da Ros, M. Prato, D. M. Guldi, E. Alessio, M. Ruzzi, L. Pasimeni, *Chem. Commun.* **1999**, 635; d) S. R. Wilson, S. MacMahon, F. T. Tat, P. D. Jarowski, D. I. Schuster, *Chem. Commun.* **2003**, 226; e) F. D'Souza, S. Gadde, M. E. Zandler, M. Itou, Y. Araki, O. Ito, *Chem. Commun.* **2004**, 2276; f) F. D'Souza, R. Chitta, S. Gadde, M. E. Zandler, A. S. D. Sandanayaka, Y. Araki, O. Ito, *Chem. Commun.* **2005**, 1279; g) J. L. Sessler, J. Jayawickramarajah, A. Gouloumis, T. Torres, D. M. Guldi, S. Maldonado, K. J. Stevenson, *Chem. Commun.* **2005**, 1892; h) A. Trabolsi, M. Elhabiri, M. Urbani, J. L. D. de la Cruz, F. Ajamaa, N. Solladié, A.-M. Albrecht-Gary, J.-F. Nierengarten, *Chem. Commun.* **2005**, 5736; i) L. Sánchez, M. Sierra, N. Martin, A. J. Myles, T. J. Dale, J. Rebek, Jr., W. Seitz, D. M. Guldi, *Angew. Chem.* **2006**, *118*, 4753; *Angew. Chem. Int. Ed.* **2006**, *45*, 4637.

[11] a) R. Takahashi, Y. Kobuke, *J. Am. Chem. Soc.* **2003**, *125*, 2372; b) R. Takahashi, Y. Kobuke, *J. Org. Chem.* **2005**, *70*, 2745; c) C. Ikeda, A. Satake, Y. Kobuke, *Org. Lett.* **2003**, *5*, 4935.

[12] F. Hajjaj, Z. S. Yoon, M.-C. Yoon, J. Park, A. Satake, D. Kim, Y. Kobuke, *J. Am. Chem. Soc.* **2006**, *128*, 4612.

[13] Y. Kobuke, H. Miyaji, *J. Am. Chem. Soc.* **1994**, *116*, 4111.

[14] I.-W. Hwang, M. Park, T. K. Ahn, Z. S. Yoon, D. M. Ko, D. Kim, F. Ito, Y. Ishibashi, S. R. Khan, Y. Nagasawa, H. Miyasaka, C. Ikeda, R. Takahashi, K. Ogawa, A. Satake, Y. Kobuke *Chem. Eur. J.* **2005**, *11*, 3753.

[15] Y. Kuramochi, A. Satake, Y. Kobuke, *J. Am. Chem. Soc.* **2004**, *126*, 8668.

[16] a) D. Kuciauskas, P. A. Liddell, S. Lin, T. E. Johnson, S. J. Weghorn, J. S. Lindsey, A. L. Moore, T. A. Moore, D. Gust, *J. Am. Chem. Soc.* **1999**, *121*, 8604; b) A. Nakano, A. Osuka, T. Yamazaki, Y. Nishimura, S. Akimoto, I. Yamazaki, A. Itaya, M. Murakami, H. Miyasaka, *Chem. Eur. J.* **2001**, *7*, 3134; c) M.-S. Choi, T. Aida, H. Luo, Y. Araki, O. Ito, *Angew. Chem.* **2003**, *115*, 4194; *Angew. Chem. Int. Ed.* **2003**, *42*, 4060.

[17] a) J. S. Lindsey, I. C. Schreiman, H. C. Hsu, P. C. Kearney, A. M. Marguerettaz, *J. Org. Chem.* **1987**, *52*, 827; b) B. J. Littler, Y. Ciringh, J. S. Lindsey, *J. Org. Chem.* **1999**, *64*, 2864.

[18] A. Ohashi, A. Satake, Y. Kobuke, *Bull. Chem. Soc. Jpn.* **2004**, *77*, 365.

[19] R. K. R. Jetti, F. Xue, T. C. W. Mak, A. Nangia, *J. Chem. Soc. Perkin Trans. 2*, **2000**, 1223.

[20] K. Sonogashira, Y. Tohda, N. Hagihara, *Tetrahedron Lett.* **1975**, *16*, 4467.
[21] a) M. Maggini, G. Scorrano, M. Prato, *J. Am. Chem. Soc.* **1993**, *115*, 9798; b) T. Da Ros, D. M. Guldi, A. F. Morales, D. A. Leigh, M. Prato, R. Turco, *Org. Lett.* **2003**, *5*, 689.
[22] When the evaporation speed of the solvent became slow during the concentration process, the solvent tended to increase in methanol concentration, which resulted in slight dissociation of the cyclic trimer. Therefore, it is better for the evaporation process to be conducted at high speed so that the solvent composition does not change significantly.
[23] a) S. T. Nguyen, R. H. Grubbs, J. W. Ziller, *J. Am. Chem. Soc.* **1993**, *115*, 9858; b) E. L. Dias, S. T. Nguyen, R. H. Grubbs, *J. Am. Chem. Soc.* **1997**, *119*, 3887.
[24] a) J. Roovers, P. M. Toporowski, *Macromolecules* **1983**, *16*, 843; b) H. Jiang, W. Lin, *J. Am. Chem. Soc.* **2004**, *126*, 7426.
[25] O. Shoji, S. Okada, A. Satake, Y. Kobuke, *J. Am. Chem. Soc.* **2005**, *127*, 2201.
[26] In ref. [15] we reported that the compound was D_{3h}-symmetric and this has since been corrected to C_{3h}-symmetric.
[27] M. Kasha, H. R. Rawls, M. A. El-Bayoumi, *Pure Appl. Chem.* **1965**, *11*, 371.
[28] I. Yamazaki, S. Akimoto, T. Yamazaki, H. Shiratori, A. Osuka, *Acta Phys. Pol. A* **1999**, *95*, 105.
[29] D. J. Quimby, F. R. Longo, *J. Am. Chem. Soc.* **1975**, *97*, 5111.
[30] C. A. Parker, W. T. Rees, *Analyst* **1960**, *85*, 587.
[31] MATERIAL STUDIO (Version 4.1/Forcite/Force Field UNIVERSAL), Accelrys, Inc. (San Diego, CA, USA, **2001**).
[32] K. A. Connors, *Binding Constants*, Wiley, New York, **1987**, pp. 24–28.
[33] The binding constant of the monodentate pyridyl ligand (4-ethynylpyridine) was calculated to be $2\times10^{3}\,\text{M}^{-1}$ in toluene. This large binding constant ($8\times10^{8}\,\text{M}^{-1}$) between **2** and N-(**1**–Zn)$_3$ reflects three-point binding from pyridyl to the zinc(II) ion.
[34] According to the binding constant of $8\times10^{8}\,\text{M}^{-1}$ in toluene, it is estimated that 97% of **2** is bound to N-(**1**–Zn)$_3$ in an equimolar mixture of **2** and N-(**1**–Zn)$_3$ at $1.0\times10^{-6}\,\text{M}$.
[35] Benzonitrile weakly binds to **6**–Zn in toluene and the binding constant was estimated to be $\approx0.5\,\text{M}^{-1}$ in toluene from the UV/Vis titration.
[36] The titration in toluene and *o*-dichlorobenzene also showed almost complete fluorescence quenching ($\approx$98%). However, because a part of macrocycle N-(**1**–Zn)$_3$ was precipitated or adsorbed onto the quartz cell on incorporating C_{60}–Tripod, accurate binding constants could not be obtained in toluene and *o*-dichlorobenzene.
[37] A control titration experiment performed by titrating C_{60} into N-(**1**–Zn)$_3$ showed no change in the UV/Vis absorption and fluorescence measurements under the same titration conditions.
[38] The fraction of the signal at 12.3 min was separated with a preparative GPC column (JAIGEL 3H; Japan Analytical Industry) by using $CHCl_3$ as eluent, and used in the metathesis reaction with Grubbs catalyst. The MALDI-TOF mass spectrum exhibited a broad signal at around 7750 Da, which corresponded to the calculated value of the tetramer (calcd for $C_{432}H_{368}N_{64}O_{32}Zn_{12}$: 7752.9). Furthermore, the plot of retention time (12.3 min) against molecular weight was added to a calibration curve for the series of cyclic compounds (Figure 6).
[39] H. Nakagawa, K. Ogawa, A. Stake, Y. Kobuke, *Chem. Commun.* **2006**, 1560.
[40] The first oxidation potentials of the coordinated monomeric and the slipped-cofacial dimeric porphyrin in dichloromethane were estimated to be 0.60 and 0.63 V, respectively, see: a) H. Ozeki, A. Nomoto, K. Ogawa, Y. Kobuke, M. Murakami, K. Hosoda, M. Ohtani, S. Nakashima, H. Miyasaka, T. Okada, *Chem. Eur. J.* **2004**, *10*, 6393; b) D. Kalita, M. Morisue, Y. Kobuke, *New J. Chem.* **2006**, *30*, 77; furthermore, the electrochemical interaction of the porphyrins through the *m*-phenylene linker could be ignored, and therefore, both the dimeric and monomeric porphyrin units in the composite C_{60}–Tripod/N-(**1**–Zn)$_3$ would have similar oxidation potentials, see: c) J. L. Sessler, M. R. Johnson, S. E. Creager, J. C. Fettinger, J. A. Ibers, *J. Am. Chem. Soc.* **1990**, *112*, 9310.
[41] Both absorption and fluorescence spectra of the monomeric porphyrins were shifted towards longer wavelengths by complexation of ligands, and approached those of the slipped-cofacial dimeric porphyrin. Thus, the energy gaps between the lowest excited state and the ground state of the coordinated monomeric and the complementary coordinated dimeric porphyrins became almost the same (2.02 eV for **6**–Zn/Im and 2.00 eV for N-(**5**–Zn)$_2$, Table 1).
[42] J.-L. Hou, H.-P. Yi, X.-B. Shao, C. Li, Z.-Q. Wu, X.-K. Jiang, L.-Z. Wu, C.-H. Tung, Z.-T. Li, *Angew. Chem.* **2006**, *118*, 810; *Angew. Chem. Int. Ed.* **2006**, *45*, 796.
[43] a) D. M. Guldi, A. Hirsch, M. Scheloske, E. Dietel, A. Troisi, F. Zerbetto, M. Prato, *Chem. Eur. J.* **2003**, *9*, 4968; b) V. Chukharev, N. V. Tkachenko, A. Efimov, D. M. Guldi, A. Hirsch, M. Scheloske, H. Lemmetyinen, *J. Phys. Chem. B* **2004**, *108*, 16377.
[44] We also attempted to determine the CT absorption and emission bands on the steady-state spectra. However, the CT bands were not observed because their signals were very weak and the noninteracting porphyrins of N-(**1**–Zn)$_3$ hid them.
[45] L. Yu, J. S. Lindsey, *J. Org. Chem.* **2001**, *66*, 7402.
[46] T. Nakamura, M. Fujitsuka, Y. Araki, O. Ito, J. Ikemoto, K. Takamiya, Y. Aso, T. Otsubo, *J. Phys. Chem. B* **2004**, *108*, 10700.

Received: November 1, 2007
Published online: January 28, 2008

